

Influence of Sm doped ZnO nanoparticles with enhanced photoluminescence and antibacterial efficiency

A. T. Ravichandran¹ · R. Karthick¹ · A. Robert Xavier¹ · R. Chandramohan² · Srinivas Mantha³

Received: 19 October 2016 / Accepted: 6 January 2017 / Published online: 25 January 2017
© Springer Science+Business Media New York 2017

Abstract Samarium doped Zinc Oxide nanoparticles are prepared by using soft chemical route with different doping concentrations. The structural studies indicated that doping does not affect the structure of ZnO lattice. The shape and size of the nanoparticles are analyzed using the FESEM and TEM images. The photoluminescence spectrum shows the increases in the intensity of violet and blue emission peaks as the concentration of dopant increases. Antibacterial activities against *Staphylococcus aureus* (*S. Aureus*) and *Escherichia coli* (*E. coli*) bacterial strains using the agar well diffusion method were studied. The increased diameter of the zone of inhibition at the higher concentration of samarium shows the enhanced efficiency of antibacterial activity.

1 Introduction

A new perspective has acquired over the past years in the field of science and technology of nanomaterials. Applications such as optical coatings, solid state window layer, electro-optical modulators and other light emitting materials are extensively being studied by II–VI compound semiconductors. In the recent decade, one of the most significant challenges is due to infectious diseases and bacterial or fungal contamination in all kinds of materials. In order to

prevent them several antibacterial and antifungal agents are widely used for the public health issues [1]. The new materials with antibacterial or antifungal properties are much needed as they have their ability which depends on the size, structure and surface properties of the nanomaterials [2].

Several metal oxides such as TiO₂, ZnO, and CuO have gained much attention of the researchers in the fields. Among them, ZnO is a promising II–VI group semiconductor material, which has direct band gap of about 3.37 eV. Also, it absorbs UV radiation due to band to band transition and it is a good transparent conductive oxide (TCO) material which are mainly for solar cells, LED and heat mirror applications [3, 4]. Above all oxide materials, ZnO is one of the most promising material due to its optical, electrical, chemical and mechanical property. Unlike the materials IFO & SnO₂, the semiconductor materials ZnO is abundant in nature, inexpensive, chemically stable, non-toxic and biocompatible [5].

Several synthesis routes have been employed to improve the performance of ZnO. Synthesis routes such as sol–gel technique [6], combustion method [7], polyol method [8], sonochemical method [9], hydrothermal method [10] and simple soft chemical route [11, 12] have been employed to improve the performance of ZnO nanoparticles.

Among all the methods, simple soft chemical route offers good tailoring of the size, and morphology of the nanoparticles. It is also very fascinating, facile and inexpensive method which is suitable for the nano structured materials in large scale [13]. Recent research has been on doping of rare-earth metal with the metal oxide semiconductors due to their unique applications in visible light emitting phosphorous in displays, high power lasers, and other opto-electronic applications. It is because, Nair.et.al reported that they have partially filled 4 f shells, and if incorporated into suitable materials, their infra-4 f optical

✉ A. T. Ravichandran
atrnc@gmail.com

¹ PG & Research Department of Physics, National College (Autonomous), Tiruchirappalli 620001, India

² PG & Research Department of Physics, Sree Sevugan Annamalai College, Devakkottai 630303, India

³ IEEE communications society, Hyderabad 500055, India

transitions become possible because of splitting induced by the crystal field in the matrix [14]. Liu et al. reported Nd^{3+} into ZnO and studied its luminescence properties [15] and Karthikeyan et al. reported linear and nonlinear optical properties of Dy^{3+} doped ZnO nanoparticles [16]. In order to increase the carrier concentration samarium is added as the dopant. Also, Sm^{3+} has a standard has an ionic radius of 1.04 Å which is appreciably higher than that of Zn which is 0.74 Å [17]. In this paper, we have extensively reviewed the effects of antibacterial efficiency and photoluminescence property of rare-earth (Sm) doped ZnO nanoparticles. To the best of our knowledge, this is the first report on the work of Sm doped ZnO nanoparticles synthesized by simple soft chemical route for biomedical applications.

2 Experimental details

2.1 Synthesis process

ZnO:Sm nanoparticles were synthesized using a simple soft chemical route. Zinc Acetate dihydrate (0.2 M) was dissolved in de-ionized water. Samarium nitrate was used as a dopant precursor with various concentrations as 2, 4, 6 at.% respectively. A suitable amount of sodium hydroxide (NaOH) solution was added to keep the pH of the starting solution at 7. The obtained mixture solution is stirred for 2 h under the temperature of 85 °C. The precipitate formed is separated out carefully by filtration and washed several times thoroughly with a mixture of ethanol and water in the ratio 1:3. The product is then dried in an oven at a temperature of 100 °C for 2 h and the powder finally calcined at 550 °C for 3 h to get the ZnO nanoparticles in its final form.

2.2 Characterization of Bi doped ZnO nanoparticles

The structural properties of synthesized nanoparticles were obtained using X-ray diffractometer (PANalytical-PW 340/60 X'pert PRO) with Cu-K α radiation (1.5406 Å). Photoluminescence (PL) spectra were studied using Spectrofluorometer (JobinYvon FLUOROLOG-FL3-11). Morphology of the sample was observed using Field Emission Scanning Electron Microscope (FESEM) (Hitachi SU8000), Transition Electron Microscopy (TEM, Hitachi H-7100) and the elemental composition analyses were made using Energy Dispersive X-ray analysis (EDX) (Model: JEOL-JSM 6390 with attachment INCA-Penta FETX3 OXFORD).

2.3 Antibacterial activity

The antibacterial activity of the synthesized ZnO nanoparticles was tested against *Staphylococcus aureus* (*S. Aureus*) (Gram-positive) and *Escherichia coli* (*E. coli*)

(Gram-negative) bacteria using the well diffusion method. The both microorganisms were inoculated on Luria broth (LB) agar plate, and then the concentration of Sm:ZnO nanoparticles (200 $\mu\text{L}/\text{mL}$) were added to the well present in the LB agar plate. A reaction mixture containing no ZnO nanoparticles was put in the well in the LB plate and cultured under the same condition as the control test. All the LB plates were incubated at 37 °C overnight. After incubation, the plates were observed in the presence of a zone of inhibition.

3 Results and discussions

3.1 X-ray diffraction (XRD) analysis

Figure 1 shows the X-ray diffraction pattern of the undoped and Sm doped ZnO nanoparticles. All the diffraction peaks are well matched with JCPDS card (34-1451) which confirms the hexagonal wurtzite structure of ZnO nanoparticles. No other peaks such as metallic zinc and ZnO_2 phase were observed. The intensity of the peaks is found to be decreased as the concentration of Sm is increased. Furthermore, the diffraction peaks of Sm doped ZnO nanoparticles, indicating the substitution of Sm^{3+} ions into the Zn^{2+} sites in the lattice of ZnO because, the ionic radius of Sm is little larger than that of Zn.

The particle size was calculated using Scherr's formula [18],

$$D = K\lambda/\beta\cos\theta \quad (1)$$

where λ is wavelength of X-ray used (1.5406 Å), β is the (101) Full-width Half maximum (FWHM) intensity and θ is the angle of the diffraction.

The lattice constant 'a', and 'c' are calculated using the relation [19],

$$1/d^2 = (4/3(h^2 + hk + k^2)/a^2) + (l^2/c^2) \quad (2)$$

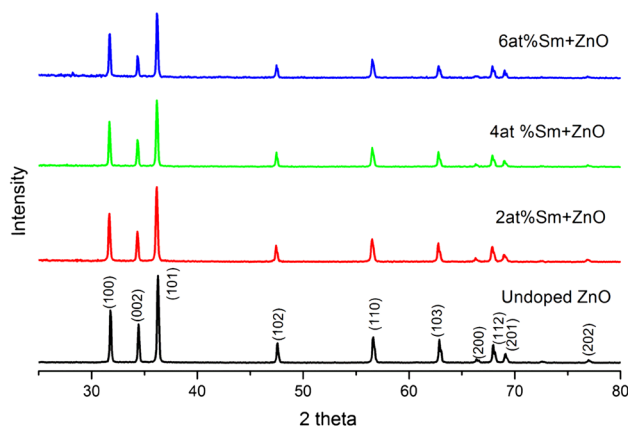


Fig. 1 XRD patterns of undoped and Sm doped ZnO nanoparticles

The volume of the unit cell (v) is calculated using the Equation [20],

$$V = \sqrt{3/2} (a^2c) \tag{3}$$

Micro strain of the nanoparticles were calculated using the formula [21],

$$\epsilon = (C - C_0/C_0) \tag{4}$$

The calculated lattice parameters and particle size of the nanoparticles are listed in Table 1. The average particle size decreases as Sm concentration increases, which is possibly due to the interference of the Sm cation to the ZnO lattice. The calculated lattice parameters ‘a’ and ‘c’ values show small variations as the doping level increases, which is due to the substitutional incorporation of Sm³⁺ ions into the ZnO lattice. The undoped ZnO clearly shows the compressive strain, whereas the doped ZnO samples exhibit tensile strain. The compressive strain created in the former may be due to the oxygen vacancies in the lattice. The transition from the compressive strain to the tensile strain may be due to the incorporation of the Sm ions into the ZnO lattice either by substitution, interstitial and/or anti-site incorporation.

3.2 Morphology and EDX

The FESEM images of undoped and Sm doped ZnO nanoparticles were shown in Fig. 2. These images clearly show that the average particle size is of the order of nano region. The average particle size decreases with the increase of the Sm concentration in ZnO lattice. This smaller particle more readily allows them to interact and penetrate to the interior of the bacteria by destroying it. The particle size is also evidenced from the TEM image Fig. 3b. From the TEM image, no aggregate is observed, in addition, no impurities have been found in ZnO material. The EDX spectra of the undoped and Sm doped ZnO nanoparticles are shown in Fig. 3a. The components present in the synthesized nanoparticles were confirmed by the presence of Zn, O, and Sm atoms.

3.3 Photoluminescence

Figure 4 shows the photoluminescence spectra of undoped and Sm doped ZnO nanoparticles. A strong emission peak at 397 and 420 nm is absorbed. There is a gradual increase of intensity as the dopant level increases. The blue emission band at centered at 420 nm may be originated from the reconstruction of the photogenerated hole with an electron occupying the oxygen vacancy. The strong peak at around 420 nm is assigned to the zinc interstitials (Zn_i) [22]. It is observed that the broad emission peak in the visible region, centered at 397 nm is associated with the near band-edge emission (NBE) of ZnO results due to the band to band electronic transition [23–26].

The variation of the emission intensity in Sm content could be ascribed to the variation of the average particle size with Sm content. The peak at 466 nm is associated with the blue emission that originates from the transition of electrons from the donor level of singly ionized oxygen vacancies to the valence band [27]. The presence of excess surface defects leads to the stronger blue emission corresponding to the formation of hydroxyl radicals [28]. These hydroxyl radicals are responsible for the inhibition of bacterial growth.

3.4 Antibacterial efficiency

The antibacterial activity of ZnO and Sm doped ZnO nanopowders were investigated against gram negative (*E. Coli*) and Gram positive (*S. Aureus*) bacteria respectively. From the Fig. 5 it is observed that there is no zone of inhibition over the control. The variation in the diameter of the zone of inhibition is plotted as a bar diagram (Fig. 6). It is observed that Sm influences the higher antibacterial activity than that of the undoped ZnO nanoparticle. This increase in the efficiency of the antibacterial activity may be due to the following reasons (i) the generation of reactive oxygen species (ROS) (ii) size of the particle (iii) release of Zn²⁺ ions. Release of more number of Zinc ions is induced in the system as the substitution of Sm ions into the Zn sites results in a larger number of Zn interstitials. It is well known that interstitial Zn ions have more probability to become free

Table 1 Structural parameters of undoped and Sm doped ZnO nanoparticles

Sm doping level (at.%)	2θ	D (nm)	*Lattice constants (Å)		v (Å) ³	Strain ε × 10 ⁻⁴
			a	c		
0	36.284	56.04	3.270	5.211	47.606	9.604
2	36.204	56.79	3.256	5.218	49.032	0.235
4	36.188	42.59	3.258	5.220	47.990	0.026
6	36.178	42.60	3.260	5.223	48.079	0.331

*Standard values: a=3.2498 Å, c=5.2066 Å (JCPDSCardNo. 36-1451)

2θ bragg’s angle, D crystallite size, v volume of the unit cell and ε micro strain

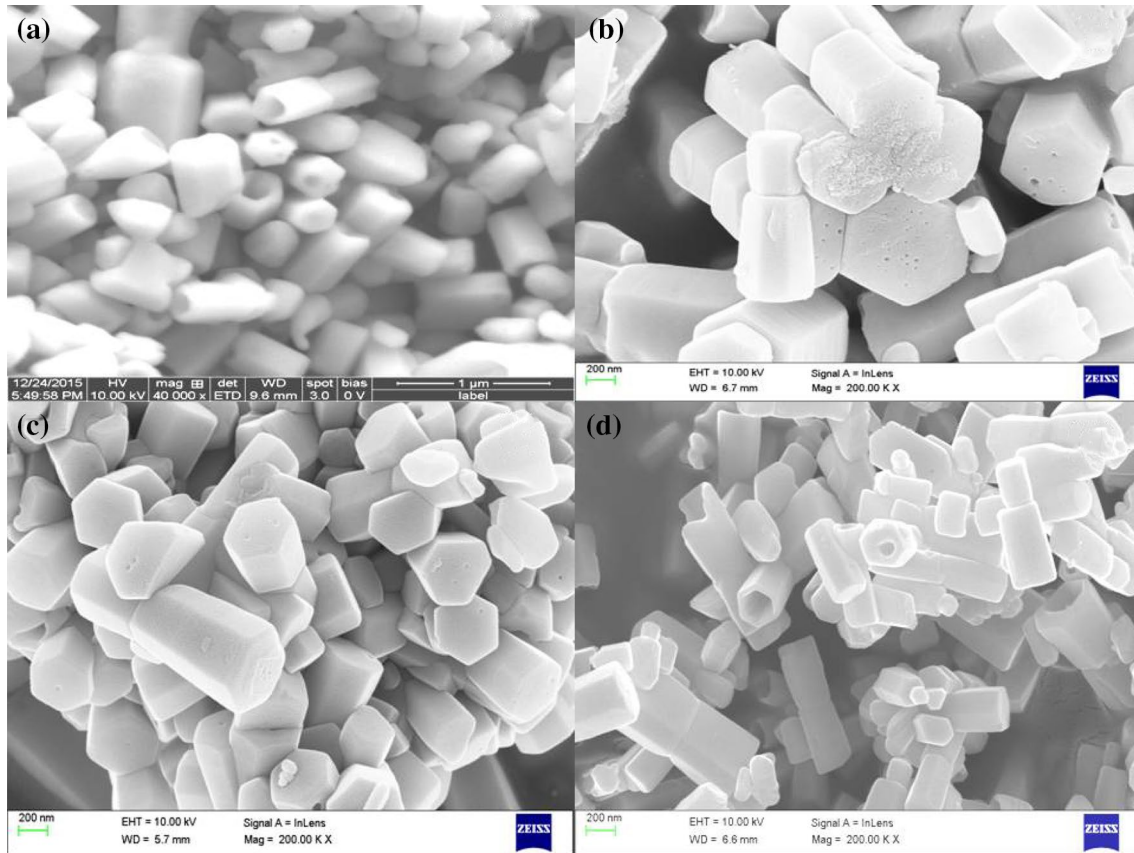


Fig. 2 FESEM images of undoped and Sm doped ZnO nanoparticles **a** undoped, **b** 2 at.%, **c** 4 at.% and **d** 6 at.%

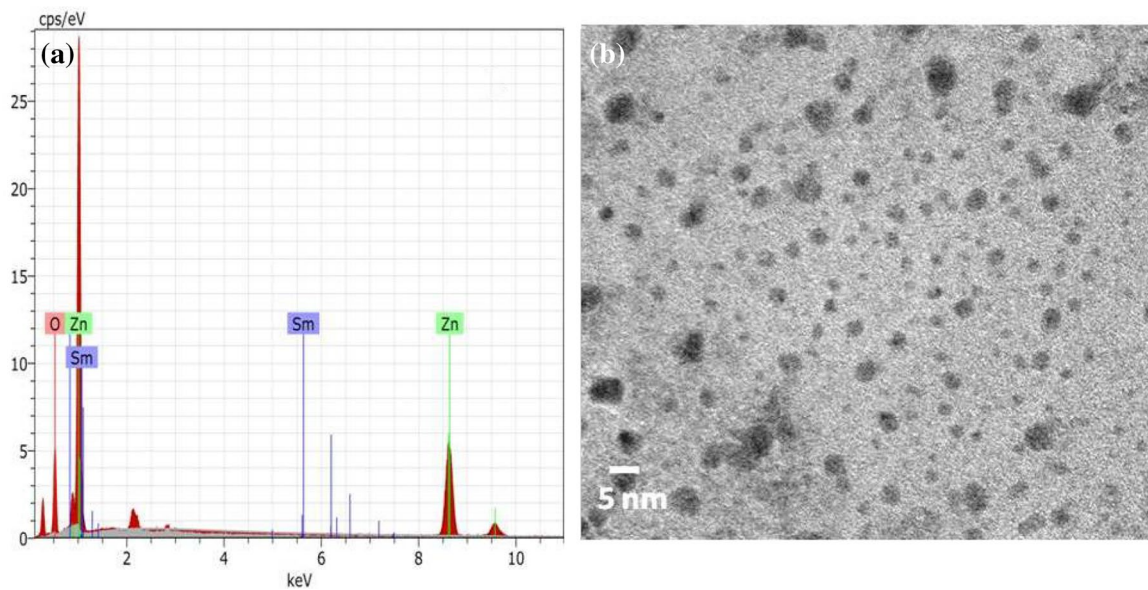


Fig. 3 **a** EDAX profile of 6 at.% Sm :ZnO, **b** TEM image of undoped ZnO nanoparticles

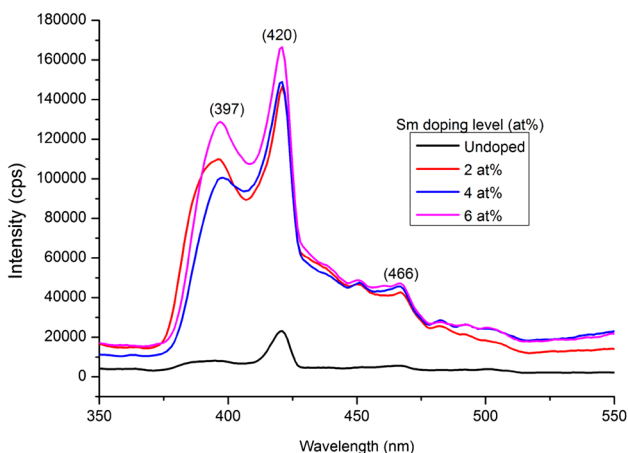
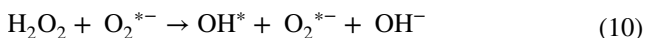


Fig. 4 Photoluminescence spectra of undoped and Sm doped ZnO nanoparticles

from the lattice. This released Zn^{2+} ions have strong electrostatic interaction with the membranes of bacteria cells, leading to a considerable damage to the bacterial cell. This generation of ROS can be written as follows [29–32]:



When compared with the hydroxyl radicals and superoxide anions, hydrogen peroxide is more toxic so that it can easily damage the cell wall of the bacteria. The peak

observed at 466 nm at the PL spectra is the evidence for the presence of singlet oxygen. This singlet oxygen is produced in the presence of superoxide anion by hydrogen peroxide which is more toxic than it. The presence of ionized vacancy is evidenced from the observed peak centered at 466 nm in the PL spectra. The release of Zn^{2+} ions is also one of the reasons for the efficiency of antibacterial activity. It is noteworthy to mention here that the antibacterial efficiency is found to be higher than that of the undoped when the Sm doping level was at 6 at%.

4 Conclusion

Undoped and Sm doped ZnO nanoparticles have been successfully prepared by simple soft chemical route. These ZnO nanoparticles were demonstrating antibacterial

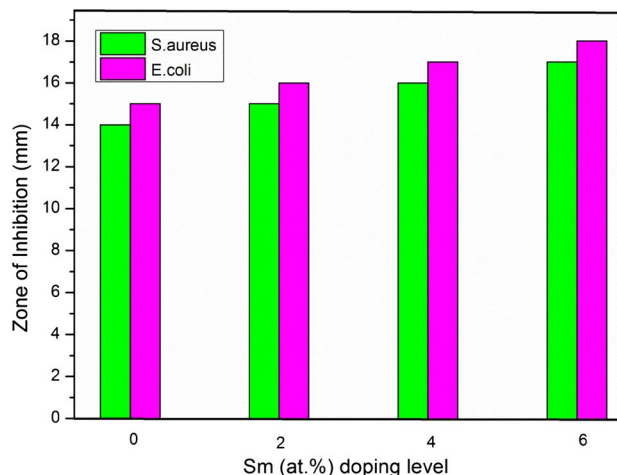
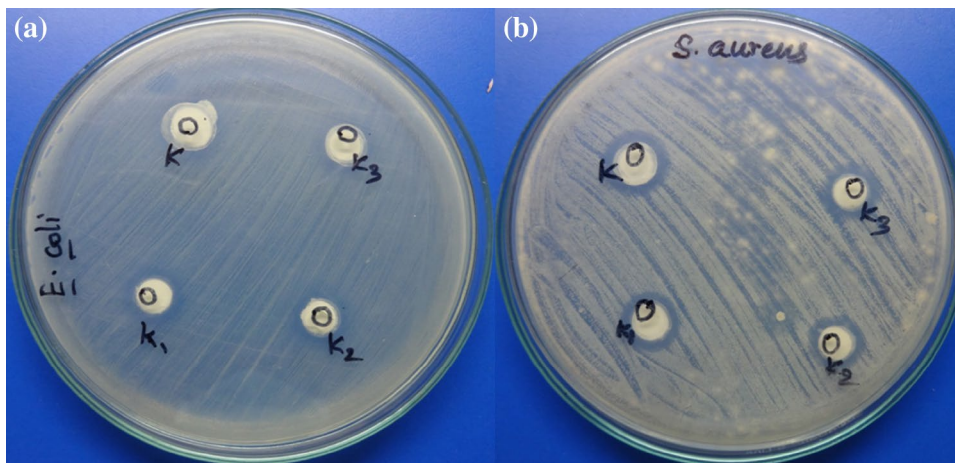


Fig. 6 Variation in the zone of Inhibition caused by ZnO+Sm nanoparticles

Fig. 5 Antibacterial activity of ZnO:Sm nanoparticles against **a** *E. coli* and **b** *S. aureus* bacteria



activity with the model bacterial the *E. coli* and *S. aureus*. The zone of inhibition increases as the dopant concentration is increased. The antibacterial activity of ZnO nanoparticles was apparent from the zone of inhibition so these nanoparticles are bellowed to act as preventive for bacterial contamination. An effect and effectiveness in changing bacterial growth, a finding which may be lead to valuable invention in the future in various fields like in antimicrobial systems as well as medical devices.

References

1. J.S. Kim, E. Kuk, K.N. Yu, J.H. Kim, S.J. Park, H.J. Lee, S.H. Kim, Y.K. Park, Y.H. Park, C.Y. Hwang, Y.K. Kim, Y.S. Lee, *Nanomedicine* **3**, 95–101 (2005)
2. K.R. Raghupathi, R.T. Koodali, A.C. Manna, *Langmuir* **27**, 4020–4028 (2011)
3. B.J. Lokhande, M.D. Uplane, *Appl. Surf. Sci.* **167**, 243 (2000)
4. E. Fortunato, P. Barquinha, A. Pimentel, L. Pereira, A. Goncalves, A. Marques, R. Martins, *Appl. Phys. Lett.* **85**, 2541 (2004)
5. A. Ashour, M.A. Kaid, N.Z. El-Sayed, A.A. Ibrahim, *Appl. Surf. Sci.* **252**, 7844–7848 (2006)
6. A. Azam, F. Ahmed, N. Arshi, M. Chaman, A.H. Naqvi, *J. Alloys Compd.* **496**, 399–402 (2010)
7. D. Sharma, S. Sharma, B.S. Kaith, J. Rajput, M. Kahn, *Appl. Surf. Sci.* **257**, 9661–9672 (2011)
8. S. Lee, S. Jeong, D. Kim, S. Hwang, M. Jeon, J. Moon, *Superlatt. Microstruct.* **43**, 330–339 (2008)
9. A.K. Zak, W.H.A. Majid, H.Z. Wang, R. Yousefi, A.M. Golsheikh, Z.F. Ren, *Ultrason. Sonochem.* **20**, 395–400 (2013)
10. S.D. Gopal Ram, G. Ravi, M.R. Manikandan, T. Mahalingam, M.A. Kulandainathan, *Superlatt. Microstruct.* **50**, 296–302 (2011)
11. K. Saravanakumar, K. Ravichandran, *J. Mater. Sci.* **23**, 1462–1469 (2012)
12. K. Saravanakumar, B. Sakthivel, K. Ravichandran, *Mater. Lett.* **65**, 2278–2280 (2011)
13. K. Saravanakumar, K. Ravichandran, R. Chandramohan, S. Gobalakrishnan, M. Chavali, *Superlatt. Microstruct.* **52**, 528–540 (2012)
14. K.G. Nair, K.P. Mani, V. George, P. Chandran, C. Josepha, V.P.N. Nampoore, Nonlinear optical characterization of samarium doped zinc oxide nanoparticles, proceedings of national laser symposium (NLS-21), (BARC, Mumbai Feb 2013), pp. 6–9
15. Y. Liu, W. Luo, R. Li, X. Chen, *J. Nanosci. Nanotech.* **10**, 1871–1876, (2010)
16. B. Karthikeyan, C.S. Suchand Sandeep, T. Pandiyarajan, P. Venkatesan, R. Philip, *Appl. Phys. A* **102**, 115–120 (2011)
17. A.R. Xavier, A.T. Ravichandran, K. Ravichandran, Srinivas Mantha, D. Ravinder, Sm doping effect on structural, morphological, luminescence and antibacterial activity of CdO nanoparticles, *J. Mater. Sci.* (2016) doi:[10.1007/s10854-016-5237-3](https://doi.org/10.1007/s10854-016-5237-3)
18. G.K. Mani, J.B.B. Rayappan, A highly selective room temperature ammonia sensor using spray deposited zinc oxide thin film. *Sens. Actuators B* **183**, 459–466 (2013)
19. K. Ravichandran, S. Snega, N. Jabena Begum, K. Swaminathan, B. Sakthivel, L. Rene Christena, G. Chandramohan, S. Ochiaie, Enhancement in the antibacterial efficiency of ZnO nanopowders by tuning the shape of the nanograins through fluorine doping. *Superlatt. Microstruct.* **69**, 17–28 (2014)
20. A. Goswami, *Thin film fund., New Age International.* ((P) Limited, Publications, New Delhi, 2005)
21. L. Ae, D. Kieven, J. Chen, R. Klenk, T. Rissom, *Prog. Photovolt.* **18**, 209–213 (2010)
22. R. Mohan, K. Ravichandran, A. Nithya, K. Jothivenkatachalam, C. Ravidhas, B. Sakthivel, Influence of spray flux density on the photocatalytic activity and certain physical properties of ZnO thin films, *J. Mater. Sci.* **25**, 2546–2553 (2014)
23. M. Wraback, H. Shen, S. Liang, C.R. Gorla, Y. Lu, High contrast ultrafast optically addressed ultraviolet light modulator based upon optical anisotropy in ZnO films grown on R-plane sapphire. *Appl. Phys. Lett.* **74**, 507 (1999)
24. D.M. Schaadt, O. Brandt, S. Ghosh, T. Flissikowski, U. Jahn, H.T. Grahn, Polarization-dependent beam switch based on an M-plane GaN/AlN distributed Bragg reflector. *Appl. Phys. Lett.* **90**, 231117 (2007)
25. P.-S. Xu, Y.-M. Sun, C.-S. Shi, F.-Q. Xu, H.-B. Pan, The electron structures of ZnO and its defects. *Sci. Chin. A.* **31**(4), 358–365 (2001)
26. B.-X. Lin, Z.-X. Fu, Green luminescent center in undoped zinc oxide films deposited on silicon substrates. *Appl. Phys. Lett.* **79**, 943–945 (2001)
27. R. Mariappan, V. Ponnuswamy, P. Suresh, *Superlatt. Microstruct.* **52**, 500–513 (2012)
28. N. Talebian J. Photochem. Photobiol. B. **120**, 66–73 (2013)
29. N.J. Begum, K. Ravichandran, *J. Phy. Chem. Solids.* **74**, 841–848 (2013)
30. A.T. Ravichandran, K.C.S. Pushpa, K. Ravichandran, K. Karthika, B.M. Nagabhushana, Srinivas Mantha, K. Swaminathan, *Superlatt. Microstruct.* **75**, 533–542 (2014)
31. K. Ravichandran, K. Karthika, M. Baneto, K. Shanthakumari, K.C. Lalithambika, *J. Mater. Sci.* **26**, 1812–1819 (2015)
32. S. Nair, A. Sasidharan, V.V.D. Rani, D. Menon, S. Nair, K. Manzoor, S. Raina, *J. Mater. Sci.* **20**, S235–S241 (2009)